Characterizing tumor-promoting T cells in chemically induced cutaneous carcinogenesis

Scott J. Roberts*, Bernice Y. Ng*, Renata B. Filler*, Julia Lewis*, Earl J. Glusac*, Adrian C. Hayday†, Robert E. Tigelaar*, and Michael Girardi*‡

*Department of Dermatology, Yale University School of Medicine, New Haven, CT 06520-8059; and †Peter Gorer Department of Immunobiology, King's College School of Medicine at Guy's Hospital, London SE1 9RT, United Kingdom

Edited by James P. Allison, Memorial Sloan–Kettering Cancer Center, New York, NY, and approved February 5, 2007 (received for review June 14, 2006)

There is a longstanding but poorly understood epidemiologic link between inflammation and cancer. Consistent with this, we previously showed that $\alpha\beta$ T cell deficiency can increase resistance to chemical carcinogenesis initiated by 7,12-dimethylbenz[*a*]anthracene and promoted by phorbol 12-myristate 13-acetate. This provoked the hypothesis that $\alpha\beta$ T cell deficiency removed T regulatory cells that limit the anti-tumor response or removed a specific tumor-promoting (T-pro) T cell population. Here we provide evidence for the latter, identifying a novel $CD8^+$ subset that is a candidate for T-pro cells. We demonstrate that CD8 cell-deficient mice show substantially less tumor incidence and progression to carcinoma, whereas susceptibility is restored by $CD8^+$ cell reconstitution. To characterize the putative T-pro cells, tumor-infiltrating lymphocytes were isolated from normal and $CD4^{-/-}$ mice, revealing an activated population of T cell receptor $\alpha\beta^+CD8^+CD44^+CD62L^-$ cells expressing the inflammatory mediators IFNγ, TNFα, and cyclooxygenase-2, but deficient in perforin, relative to recirculating cells of equivalent phenotype. This novel population of $CD8^+$ T cells has intriguing similarities with other lymphocytes that have been associated with tissue growth and invasiveness and has implications for inflammation-associated carcinogenesis, models of cancer immunosurveillance, and immunotherapeutic strategies.

inflammation | IFNγ | squamous cell carcinoma | T cell receptor

Epithelial tissues, situated at the critical juncture of the host with its environment, are continually subjected to myriad damaging factors that provoke inflammation including chemical toxins and mutagens, proliferation-inducing factors, and infectious agents. Numerous correlations of such inflammatory states with increased carcinogenesis have been identified, e.g., cutaneous squamous cell carcinoma (chronic cutaneous lupus, cutaneous tuberculosis, chronic wounds/ulcers), lung carcinoma (asbestos and silica exposure), gastric carcinoma (*Helicobacter pylori* associated gastritis), esophageal carcinoma (Barrett's esophagitis), and colorectal carcinoma (inflammatory bowel disease) (reviewed in ref. 1). Indeed, the "chronic inflammatory state" has long been postulated (2) to drive recurrent rounds of epithelial damage and repair, with associated local increased oxidative stress, secretion of growth factors, and cell cycle dysregulation. This would provide a microenvironment conducive to mutagenesis and genomic instability, which are fundamental to carcinogenesis (3).

Analysis of most sporadic premalignant tumors and carcinomas arising in adults commonly reveals numerous leukocytes and prominent production of inflammatory cytokines including IFNγ and TNFα (4). Whereas IFNγ is known to exhibit a wide variety of effects antagonistic to tumor development and growth (e.g., inhibition of angiogenesis, up-regulation of antigen presentation, enhancement of cytotoxic responses, granulomatous control of tumors) (5, 6), locally sustained IFNγ expression has been paradoxically implicated in enhancing tumor progression (7, 8). Likewise, TNFα may induce focal tumor cell death and stimulate anti-tumor responses but is commonly present in chronic inflammatory states and their associated carcinomas (9, 10). Nonetheless, the cutaneous inflammatory condition psoriasis, notable for local TNFα production, is one state where inflammation itself has no apparent influence on skin cancer development (11). Thus, specific cellular components that drive inflammation, rather than inflammation *per se*, are likely to be key to promoting carcinogenesis, and their identification by use of experimental systems is therefore an important goal.

Accordingly, we used a two-stage chemical carcinogenesis protocol of single exposure to the mutagen 7,12-dimethylbenz[*a*]anthracene (DMBA) followed by repeated application of the inflammation-inducing phorphol ester, phorbol 12-myristate 13-acetate (PMA), where lesions can be followed from premalignant papilloma formation to progression to carcinoma (12). Although the effects of PMA are pleiotropic, that its pro-inflammatory effects are crucial to tumor promotion is well supported by several major lines of evidence, most notably genetic (13, 14) and pharmaceutical (15, 16) manipulation of the arachidonic acid/cyclooxygenase (COX) pathway of inflammation induction.

Using this system we previously demonstrated that $\alpha\beta$ T cell deficiency was associated with reduced tumor development and progression in DMBA/PMA chemical carcinogenesis (17, 18). This was in contrast to $\gamma\delta$ T cell deficiency that was reproducibly deleterious to tumor resistance (18). These findings provoked two possible explanations: According to one scenario, $\alpha\beta$ T cell deficiency removes a population of T regulatory cells that ordinarily limit innate and adaptive components of the anti-tumor response (19, 20). Such would include $CD4^+CD25^+Foxp3^+$ T regulatory cells, currently a major target in clinical studies aimed at increasing the anti-tumor response (21). In addition, it would include $CD4^+$ T cell inhibition of cell-mediated anti-tumor immunity through misdirected (i.e., T helper 2 type) cytokine production, e.g., reactive against colonizing staphylococcal antigens (22), or after anti-tumor vaccination (23). Moreover, because $\gamma\delta$ T cells do not include $Foxp3^+$ regulatory cells (24), $\gamma\delta$ T cell deficiency would not be expected to have an equivalent effect. However, according to the alternative possibility, $\alpha\beta$ T cell deficiency removes a putative subset of tumor-promoting T cells (T-pro cells) that promotes inflammation associated cancer.

This article examines these two scenarios. Whereas tumor studies in $CD4^{-/-}$ mice provided little support for a prominent role of T regulatory cells, we were able to identify a putative T-pro tumor-

Author contributions: S.J.R. and B.Y.N. contributed equally to this work; A.C.H., R.E.T., and M.G. designed research; S.J.R., B.Y.N., R.B.F., J.L., E.J.G., R.E.T., and M.G. performed research; S.J.R., B.Y.N., R.B.F., and M.G. analyzed data; and S.J.R., B.Y.N., R.B.F., A.C.H., R.E.T., and M.G. wrote the paper.

The authors declare no conflict of interest.

This article is a PNAS Direct Submission.

Abbreviations: DMBA, 7,12-dimethylbenz[*a*]anthracene; PMA, phorbol 12-myristate 13-acetate; T-pro T, tumor-promoting T; TCR, T cell receptor; COX, cyclooxygenase; TIL, tumor-infiltrating lymphocyte; PBL, peripheral blood lymphocyte; NK, natural killer; FasL, Fas ligand; qRT-PCR, quantitative RT-PCR; sqRT-PCR, semiquantitative RT-PCR; SLN, spleen and lymph node; FLHC, fetal liver hematopoietic cell.

‡To whom correspondence should be addressed at: Yale University School of Medicine, 333 Cedar Street, HRT 616, New Haven, CT 06520-8059. E-mail: girardi@yale.edu.

www.pnas.org/cgi/doi/10.1073/pnas.0604982104

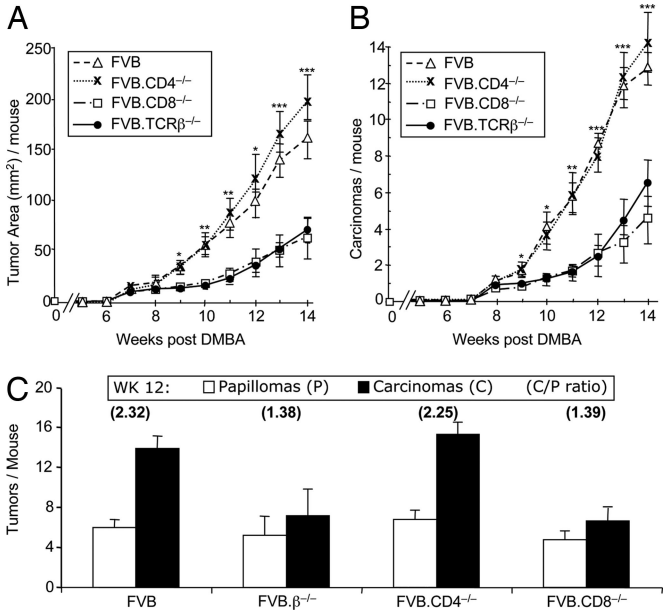

Fig. 1. Mice genetically deficient in CD8$^+$ T cells demonstrate reduced tumor development and progression. Groups of mice (n = 10) subjected to DMBA/PMA were monitored weekly for tumors. (*A*) TCR$\beta^{-/-}$ mice (deficient in both CD4$^+$ and CD8$^+$ T cells) and CD8$^{-/-}$ mice demonstrated significantly lower total tumor burden than strains in which the CD8 compartment was intact (FVB controls and CD4$^{-/-}$ mice). (*B*) Numbers of carcinomas were also substantially lessened in those mice (TCR$\beta^{-/-}$ and CD8$^{-/-}$) genetically lacking CD8$^+$ T cells. *, $P \leq 0.05$; **, $P \leq 0.01$; ***, $P \leq 0.005$ (for CD4$^{-/-}$ or FVB vs. TCR$\beta^{-/-}$ or CD8$\beta^{-/-}$). (*C*) Progression to carcinoma, as exemplified by the carcinoma/papilloma (C/P) ratio at week 12, was significantly greater in the CD8-intact mice than in the CD8-deficient mice ($P < 0.002$ for CD4$^{-/-}$ or FVB vs. TCR$\beta^{-/-}$ or CD8$\beta^{-/-}$). Error bars represent standard error of the mean.

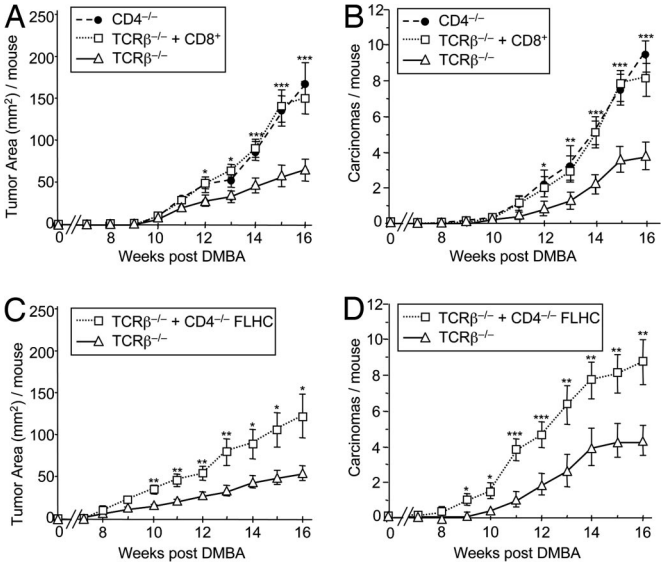

Fig. 2. Reconstitution with CD8$^+$ T cells restores the associated increased tumor susceptibility. Reconstitution of the CD8$^+$ T cell compartment of TCR$\beta^{-/-}$ mice (deficient in both CD4$^+$ and CD8$^+$ T cells) was performed in adult and neonatal recipients. (*A* and *B*) In adult TCR$\beta^{-/-}$ mice reconstituted with CD8β^+ SLN cells purified from normal FVB mice by using antibody-coated magnetic beads, tumors developed at a rate greater than that of unreconstituted TCR$\beta^{-/-}$ mice and approximately equal to that of control CD4$^{-/-}$ mice. *, $P \leq 0.05$; **, $P \leq 0.01$; ***, $P \leq 0.005$ (for CD4$^{-/-}$ or TCR$\beta^{-/-}$ plus CD8$^+$ SLN vs. TCR$\beta^{-/-}$). (*C* and *D*) Similarly, TCR$\beta^{-/-}$ mice reconstituted as neonates with FLHC progenitors from CD4$^{-/-}$ mice were more susceptible to carcinogenesis than unreconstituted TCR$\beta^{-/-}$ mice. *, $P \leq 0.05$; **, $P \leq 0.01$. Error bars represent standard error of the mean.

infiltrating lymphocyte (TIL) population, comprised of activated T cell receptor (TCR) $\alpha\beta^+$CD8$^+$CD44$^+$CD62$^-$ T cells, that produces substantial amounts of IFNγ and TNFα, but relatively little perforin, compared with phenotypically equivalent peripheral blood lymphocytes (PBL). In addition, these cells are notable for local production of COX-2, consistent with a population of CD8$^+$ T-pro cells that drives inflammatory-associated carcinogenesis in the skin. They also share intriguing similarities with uterine natural killer (NK) cells that, rather than being cytolytic, are cytokine-producing cells associated with trophoblast growth and invasion of the uterine wall (25). The identification and elucidation of mechanistic activities for tumor-promoting CD8$^+$ T cells has major implications for chemopreventive and immunotherapeutic strategies designed to enhance cancer immunosurveillance.

Results and Discussion

T-Pro Cells Are Present Within the CD8 Compartment. Groups of 10–15 age- and sex-matched mice genetically deficient in CD4 (CD4$^{-/-}$), CD8 (CD8$\beta^{-/-}$), or all TCR$\alpha\beta$ (TCR$\beta^{-/-}$) T cells, but otherwise syngeneic to the FVB strain background, were subjected to two-stage chemical carcinogenesis and compared with normal WT FVB controls. Striking parallels of increased tumor burden (Fig. 1*A*) and progression to carcinoma (Fig. 1*B*) were observed for mice in which the CD8 compartment was intact (CD4$^{-/-}$ and WT) compared with mice in which CD8 T cells were absent (CD8$\beta^{-/-}$ and TCR$\beta^{-/-}$). By experiment termination at week 14, tumor burden was ≈3-fold greater (195.6 ± 21.9 mm^2 in CD4$^{-/-}$ and 153.3 ± 18.8 in FVB vs. 54.5 ± 19.8 in TCR$\beta^{-/-}$ and 63.1 ± 12.2 in CD8$\beta^{-/-}$; $P < 0.001$), and carcinoma number was more than double (13.1 ± 0.98 in CD4$^{-/-}$ and 14.7 ± 1.8 in FVB vs. 4.0 ± 1.4 TCR$\beta^{-/-}$ and 6.2 ± 1.5 in CD8$\beta^{-/-}$; $P < 0.001$) in the CD8-intact mice relative to CD8-deficient mice. There was no significant difference between CD8$\beta^{-/-}$ and TCR$\beta^{-/-}$ mice. A comparison of the carcinoma/papilloma ratios, shown at week 12 after DMBA initiation (Fig. 1*C*), emphasizes the association of the CD8 compartment with tumor progression (1.38 for TCR$\beta^{-/-}$ and 1.39 for CD8$\beta^{-/-}$ vs. 2.25 for CD4$^{-/-}$ and 2.32 for FVB; $P < 0.002$).

In sum, the comparability of WT and CD4$^{-/-}$ mice does not imply an aggregate, substantial role for CD4$^+$ T regulatory cells in this system, but, by contrast, the decreased tumor numbers in TCR$\beta^{-/-}$ and CD8$^{-/-}$ mice strongly suggest the possibility of a population of tumor-promoting TCR$\alpha\beta^+$CD8$^+$ (i.e., T-pro) cells operative in CD8-intact mice. The possibility that other CD8-expressing (non-T) cells (e.g., dendritic cell subsets) may be partially or wholly responsible for the data is highly unlikely, because the mutation targeted the CD8β gene and CD8$^+$ dendritic cell subsets have been shown to express only the CD8$\alpha\alpha$ homodimer. Nonetheless, repopulation studies were undertaken to test the hypothesis that the tumor-promoting cells are T cells.

Selective Adult and Neonatal Repopulation Studies Confirm That T-Pro Cells Are TCR$\alpha\beta^+$CD8$^+$ T Cells. One week after initiation with DMBA, groups of TCR$\beta^{-/-}$ mice were repopulated i.v. with 3.5×10^6 CD8β^+ T cells purified from spleen and lymph node (SLN) cells by using antibody-coated magnetic beads. Just as for control CD4$^{-/-}$ mice, TCR$\alpha\beta$-deficient animals repopulated with peripheral TCR$\alpha\beta^+$CD8$^+$ T cells exhibited an increase in observed tumor burden (151.9 ± 19.6 mm^2 in TCR$\beta^{-/-}$ plus CD8$^+$ vs. 64.5 ± 13.2 in TCR$\beta^{-/-}$; $P < 0.001$) (Fig. 2*A*), and numbers of carcinomas (7.9 ± 0.92 in TCR$\beta^{-/-}$ plus CD8$^+$ vs. 3.7 ± 0.78 TCR$\beta^{-/-}$; $P = 0.001$) (Fig. 2*B*) relative to unreconstituted $\alpha\beta$ T cell-deficient mice. In a complementary experi-

IMMUNOLOGY

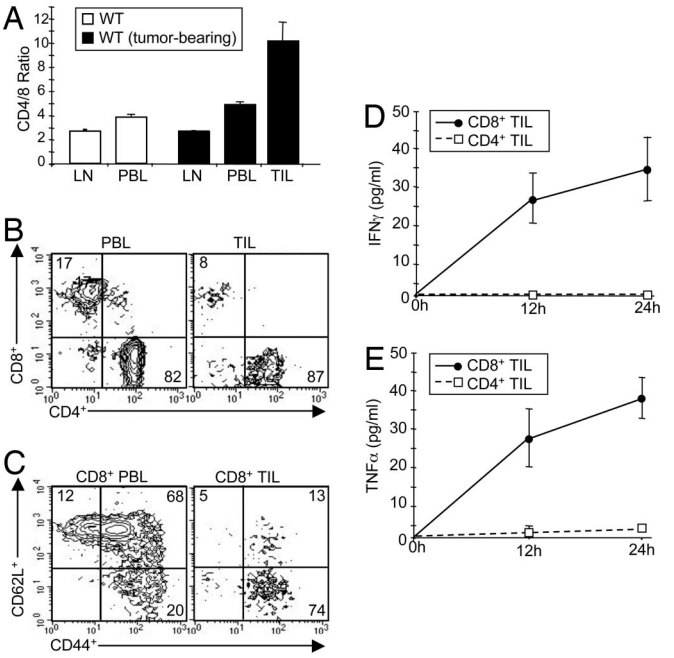

Fig. 3. CD8$^+$ TIL (putative T-pro) are activated and produce inflammatory cytokines IFNγ and TNFα. (*A*) Flow cytometric analysis of lymph node (LN), PBL, and TIL from tumor-bearing FVB control mice (filled bars) and non-tumor-bearing naïve control mice (open bars) revealed the relative CD4/CD8 ratios in each population ($n = 7$). (*B* and *C*) Representative flow cytometric analysis of lymphocytes from FVB control mice demonstrates that the vast majority of CD8$^+$ TIL are CD44$^+$CD62L$^-$, consistent with an activated effector/memory phenotype, in contrast to the peripheral blood, where only a small minority of CD8$^+$ PBL are single-positive for CD44. (Numbers represent means of five cohorts of up to five mice.) (*D* and *E*) Cytometric bead array analysis of cytokine production by TIL from normal FVB mice demonstrated substantially higher secretion by CD8$^+$, relative to equal numbers of CD4$^+$, TIL of IFNγ and TNFα.

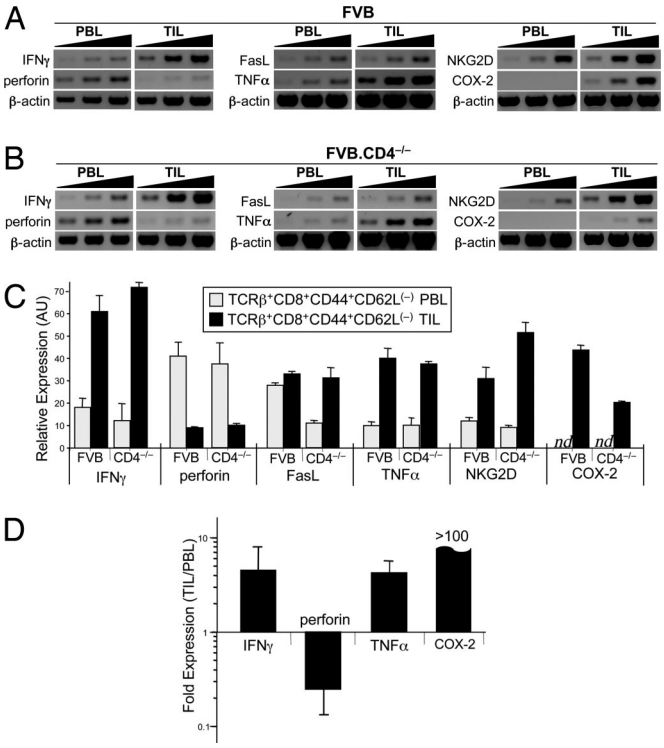

Fig. 4. RT-PCR expression analysis comparison of TCRβ^+CD8$^+$CD44$^+$CD62L$^-$ TIL vs. phenotypically equivalent PBL. Representative bands obtained from sqRT-PCR of mRNA isolated from FVB (*A*) and FVB.CD4$^{-/-}$ (*B*) mouse TIL and PBL (stained and sorted to >99.5% purity for TCR$\alpha\beta^+$CD8$^+$CD44$^+$CD62L$^-$) are shown for several inflammatory mediators (IFNγ, TNFα, and COX-2) and mediators involved in cellular killing (perforin, NKG2D, and FasL), along with control β-actin. (*C*) The mean relative expression reveals that the equivalent trends of expression (e.g., increased inflammatory mediators and decreased perforin) are consistent between PBL and TIL from FVB and FVB.CD4$^{-/-}$ mice ($P \leq 0.05$ for all comparisons). (*D*) Real-time qRT-PCR fold expression differences are shown for IFNγ, TNFα, perforin, and COX-2 when TCR$\alpha\beta^+$CD8$^+$CD44$^+$CD62L$^-$ TIL were compared with phenotypically equivalent PBL from tumor-bearing mice.

ment, neonatal TCR$\beta^{-/-}$ mice were selectively reconstituted with CD8$^+$ T cell progenitors by i.p. injection with 50,000 day-14 fetal liver hematopoietic cells (FLHC) purified from CD4$^{-/-}$ fetuses. A CD8 compartment, comparable to levels observed in CD4$^{-/-}$ mice, was confirmed in all recipients by flow cytometric analysis of PBL (data not shown). Relative to TCR$\alpha\beta$-deficient controls, the CD8-reconstituted mice again showed a significant increase in tumor burden (127.1 $\pm$ 26.9 mm^2 in TCR$\beta^{-/-}$ plus CD4$^{-/-}$ FLHC vs. 57.7 $\pm$ 9.1 in TCR$\beta^{-/-}$; $P < 0.030$) (Fig. 2*C*) and number of carcinomas (8.8 $\pm$ 1.3 mm^2 in TCR$\beta^{-/-}$ plus CD4$^{-/-}$ FLHC vs. 4.4 $\pm$ 0.86 in TCR$\beta^{-/-}$; $P < 0.010$) (Fig. 2*D*).

Phenotypic Analysis of CD8$^+$ TIL (Putative T-Pro) Associated with Increased Carcinogenesis. The prospect of a tumor-promoting TCR$\alpha\beta^+$CD8$^+$ cell population may appear paradoxical given the anti-tumor role typically attributed to perforin-producing cytotoxic CD8$^+$ T cells reactive against tumor-associated antigens (19). We therefore sought to phenotypically characterize TIL that we hypothesized contain T-pro cells that locally promote carcinogenesis. TIL purified from the tumors of DMBA/PMA treated FVB mice revealed the presence of CD3$^+$CD8$^+$ cells, albeit in much smaller numbers ($\approx$10$\times$) than CD3$^+$CD4$^+$ TIL (Fig. 3*A*). Although these cell recoveries were too low to permit the functional assay of CD8$^+$ TIL, for example by adoptive transfer, the cells could be phenotyped. They had an effector-memory, CD44$^+$CD62L$^-$ phenotype ($\approx$75% in TIL vs. $\approx$20% in PBL) (Fig. 3 *B* and *C*), and, after overnight stimulation with anti-CD3, they were shown by cytometric bead analysis to produce high amounts of IFNγ (30.0 $\pm$ 11.2 vs. 0.7 $\pm$ 1.3 pg/ml; $P = 0.002$) (Fig. 3*D*) and TNFα (31.3 $\pm$ 7.8 vs. 2.6 $\pm$ 1.7 pg/ml; $P < 0.001$) (Fig. 3*E*), relative to CD4$^+$ TIL. Consistent with this, semiquantitative RT-PCR (sqRT-PCR) analysis revealed that the TCR$\alpha\beta^+$CD8$^+$CD44$^+$CD62L$^-$ TIL also produce COX-2, the major enzymatic inducer of inflammatory mediators of the arachidonic acid pathway, whereas phenotypically equivalent PBL do not (Fig. 4 *A*–*C*). Furthermore, although the CD8$^+$ TIL express Fas ligand (FasL) and NKG2D, they conspicuously underexpress perforin. Thus, the cells compose a distinct population of CD8$^+$ T cells. To confirm findings, analyses by real-time quantitative RT-PCR (qRT-PCR) were performed to compare expression of IFNγ, TNFα, perforin, and COX-2 in TCR$\alpha\beta^+$CD8$^+$CD44$^+$CD62L$^-$ TIL relative to phenotypically equivalent PBL from tumor-bearing mice (Fig. 4*D*). Again, the inflammatory mediators were overexpressed, whereas perforin expression was substantially compromised in the putative T-pro population.

The data reported here provide further and specific support for the view that the contributions of T lymphocytes to tumor surveillance are a mixture of competing forces. On one hand, there is extensive evidence for an anti-tumor role of T cells, perhaps most obvious clinically in the increased risk of several cancers in iatrogenically immunosuppressed renal transplant patients (26). Conversely, chronic inflammation is undeniably linked to cancer in a wide variety of tissues, especially skin and other epithelia (1, 2, 4, 7–10, 13–16). Experimentally, evidence for a tumor-promoting role of T cells was first put forth by Prehn decades ago (27), with more recent findings implicating the CD4 subset (22, 23). Herein we reveal the tumor-promoting capacity

of $CD8^+$ T cells, and the aggregate expression profile of this candidate T-pro population is notably consistent with reports that $TNF\alpha^{-/-}$ (28) and $COX\text{-}2^{-/-}$ (29) mice are resistant to DMBA/PMA-mediated carcinogenesis. These data are also consistent with the recent finding of spontaneous colorectal carcinoma development in suppressor of cytokine signaling-1-deficient mice through an INFγ/STAT1-dependent pathway (30). The potential role of IFNγ in promoting inflammation-associated carcinogenesis is more enigmatic, especially given the high susceptibility of $IFN\gamma^{-/-}$, $IFNGR1^{-/-}$, and $STAT1^{-/-}$ mice to a variety of spontaneous or specific regimens of chemically induced tumors (5, 6). Nevertheless, there is also evidence that chronic, local production of IFNγ may result in a variety of pro-tumor effects (7, 8).

This pleiotropic response of T cells in the context of malignancy is reminiscent of the involvement of macrophages which are well known to include those that promote as well as those that antagonize tumor development (31). It is also reminiscent of aspects of normal physiology: thus, whereas NK cells are prototypically cytotoxic, uterine NK cells produce high amounts of cytokines, including IFNγ, but are not cytolytic and are associated with trophoblast growth and invasion of the uterus (25). This may be directly analogous to the capacity of cytokine-producing T-pro cells to promote tumor growth. Moreover, a recently identified $CD8^+$ T cell subpopulation that traffics to human skin also has a cytokine-expressing, noncytolytic phenotype similar to the candidate murine T-pro population (32). Whether such cells promote carcinogenesis in humans remains to be investigated.

Materials and Methods

Animals and Housing. All of the *in vivo* studies were approved by the Yale Animal Care and Use Committee. Normal control mice were purchased from The Jackson Laboratory (Bar Harbor, ME). $CD4^{-/-}$, $CD8\beta^{-/-}$ (both generously provided by L. Coussens, University of California, San Francisco, CA), and $TCR\beta^{-/-}$ (The Jackson Laboratory) were all backcrossed at least 10 generations onto the FVB/N background. Mice were housed in filter-topped cages with sterilized food and water and autoclaved corncob bedding changed at least once weekly. The animal facility is accredited by the Association for Assessment of Laboratory Animal Care.

Two-Stage Chemical Carcinogenesis. Chemicals were obtained from Sigma (St. Louis, MO). DMBA was dissolved in acetone (4 mM), and PMA was dissolved in 100% ethanol (0.2 mM). Application of DMBA/PMA and tumor monitoring were performed as previously described (17). Briefly, initiation by pipette application of 400 nmol of DMBA was performed 1 week after shaving back hair with electric clippers followed by depilatory cream. This was followed by twice-weekly application of 20 nmol of PMA. Cutaneous tumors were counted, measured, and scored weekly as clinically apparent papillomas (typically well demarcated, symmetrical, pedunculated or dome-shaped papules without erosion or ulceration) or clinically apparent carcinomas (poorly demarcated, asymmetrical, nonpedunculated or dome-shaped papules with erosion or ulceration). Tumors were evaluated by visual inspection by an observer (R.B.F.) blinded to the experimental groups. At the conclusion of experiments, tumors were excised for TIL isolation or formalin-fixed and paraffin-embedded, and 5-μm sections were stained with hematoxylin and eosin and examined (by E.J.G.) for histologic confirmation.

Lymphocyte Isolation. To obtain PBL samples, after anesthesia by methoxyflurane inhalation mice were individually bled by capillary pipette of the retroorbital plexus. Approximately 200 μl per mouse was harvested, mixed with 30 μl of 1,000 units/ml heparin (Sigma) and then 5 ml of D-PBS. The blood mixture was overlaid on 5 ml of Lympholyte-M (Accurate Chemical, Westbury, NY) and centrifuged at $600 \times g$ for 20 min at room temperature, and the interface was harvested and washed twice in Hanks' balanced salt solution (HBSS) before antibody staining. All mice were processed individually then either stained as individual mice or pooled and then stained for sorting. Cells were sorted on a FACSVantage with DIVA option for the cytometric bead analysis assay (see below) or sorted into individual wells of a 96-well plate (500 cells per well) on a MoFlo (DakoCytomation, Fort Collins, CO) for subsequent expression analysis (see below). To obtain SLN cells, the tissues were ground between frosted slides, and the cells were released into ice-cold HBSS and purified on Lympholyte-M columns as described above. The cells were washed twice in HBSS before sorting and transfer studies. To obtain TIL, tumors were excised and minced on ice in supplemented RPMI medium 1640 (sRPMI: RPMI medium 1640 plus Hepes, 2-mercaptoethanol, sodium pyruvate, and antibiotics) with 2.5 mg/ml collagenase I, 1.5 mg/ml collagenase II, 1 mg/ml collagenase IV, 0.25 mg/ml hyaluronidase IV-S, 300 μg/ml DNase I, and 0.06 μg/ml soybean trypsin inhibitor. Suspensions of tumor pieces were incubated at 37°C for 2 h. The pieces were then gently pressed between the frosted edges of two sterile glass slides, and the cell suspension was passed through sterile 100-μm Nylon mesh to remove debris and separate cell clumping. sRPMI was added to stop the digestion. Cells were centrifuged at 1,200 rpm at 4°C and washed three times in HBSS before Lympholyte-M gradient separation. TIL were further purified by using the gradient as per manufacturer protocol, washed three times in HBSS, and resuspended in sRPMI for overnight incubation at 37°C 5% CO_2. The following day, the TIL were washed two times in HBSS and filtered through 30-μm Nytex filter and stained. Cells were either analyzed fresh or fixed in freshly prepared 1% paraformaldehyde in PBS.

Flow Cytometry. FITC, phycoerythrin, peridinin chlorophyll protein coupled to cyanine dye (PerCPCy5.5), or allophycocyanin-conjugated monoclonal antibodies specific for CD3 (145-2C11), CD4 (RM4-5), CD8α (53-6.7), CD62L (MEL-14), TCRβ (H57-597), and CD44 (IM7) were from Pharmingen (San Diego, CA). Biotinylated CD8β (CT-CD8b) for magnetic selection was from eBiosciences (San Diego, CA). For flow cytometry, 1×10^6 PBL or TIL after purification over Lympholyte-M (PBL) or Nytex filtration (TIL) were stained for 30 min at 4°C with a 1:100 dilution for FITC-conjugated antibodies, 1:200 for phycoerythrin-conjugated antibodies, 1:150 for PerCPCy5.5-conjugated antibodies, and 1:400 for allophycocyanin-conjugated antibodies in flow cytometry buffer (2% FCS in HBSS), were washed twice with flow cytometry buffer, and were analyzed either fresh or after fixation in 1% paraformaldehyde in PBS. A total of 2×10^4 or more lymphocyte gated events were collected on a FACSCalibur (Becton Dickinson, San Diego, CA) and analyzed with CellQuest software.

Cytometric Bead Array Cytokine Analysis. TIL from WT mice were isolated and stained for CD4 (RM4-5) and CD8a (53-6.7). The sorted populations were counted and then split into two wells of a 96-well plate coated with anti-mouse CD3 containing 200 μl of serum-free AIM V defined media (Invitrogen). At 12 and 24 h after plating, 50-μl aliquots were taken and immediately frozen at −70°C until the inflammation assay was run. Following the manufacturer's instructions, samples were run on a FACSCalibur and the data were analyzed with BD Cytometric Bead Array software. Cytokine production was determined as picograms per milliliter.

FLHC Reconstitution. Newborn $TCR\beta^{-/-}$ mice were reconstituted with peripheral $\alpha\beta$ T cell progenitors from FLHC of $FVB.CD4^{-/-}$ mice as follows. Day-14 fetal livers were harvested

and gently pressed between the frosted edges of two glass slides, releasing the cells into ice-cold HBSS containing 4 mM Hepes buffer and antibiotics. Fetal liver cells were filtered through nylon mesh (Nytex cloth 88/42; Tetko), washed twice with HBSS, and resuspended at appropriate concentrations in sterile PBS before i.p. injection at 4×10^6 cells in 30 μl of PBS per newborn TCR$\beta^{-/-}$ recipient. At 6 weeks the recipients PBL were checked for the reconstitution of CD3$^+$TCR$\alpha\beta^+$CD8$^+$ cells.

Transfer of Magnetically Purified CD8β^+ SLN Cells. One week after DMBA initiation, SLN cells from FVB mice were removed and a single-cell suspension was obtained as previously described (see above). The cells were counted on a hemocytometer and stained with CD8-biotin (CT-CD8b) from eBiosciences as instructed by the Cellection Biotin Binder Kit from Invitrogen (Carlsbad, CA), followed by positive magnetic selection. Cells were enumerated and washed twice in PBS. Cell purity was verified by FACS at >95%. Mice were reconstituted with the isolated cells via i.v. injection at 4×10^5 cells in sterile PBS per TCR$\beta^{-/-}$ recipient.

sqRT-PCR and Real-Time RT-PCR Expression Analyses. Poly(A)mRNA was isolated from sorted lymphocyte populations by using the Dynabeads mRNA DIRECT Micro Kit (Invitrogen), following the manufacturer's protocol. Bead/mRNA complexes were washed twice in 100 μl of washing buffer A (10 mM Tris·HCl, 0.15 M LiCl, 1 mM EDTA, and 0.1% LiDS) followed by two additional washes in 100 μl of washing buffer B (10 mM Tris·HCl, 0.15 M LiCl, and 1 mM EDTA) and immediately used for sqRT-PCR. Relative cytokine mRNA expression was determined by reverse transcription and semiquantitative gene amplification in a one-tube format by using the SuperScript III One-Step RT-PCR System with Platinum *Taq* High Fidelity (Invitrogen). Each standard RT-PCR mixture contained template RNA (Dynabeads/mRNA complexes), 25 μl of 2× reaction mix (0.4 mM of each dNTP and 2.4 mM $MgSO_4$), 1 μl of 20 μM forward primer, 1 μl of 20 μM reverse primer, 22 μl of distilled, autoclaved ddH_2O, and 1 μl of SuperScript III RT/Platinum *Taq* High Fidelity Enzyme Mix in a total volume of 50 μl. Thermal cycling was conducted as follows: cDNA synthesis (55°C for 30 min), predenaturation (94°C for 2 min), followed by 28–40 cycles of denaturation (94°C for 15 seconds), annealing (55°C for FasL and TNFα; or 63°C for INFγ, perforin, COX-2, and NKG2D) for 30 seconds, extension (68°C for 1 min), and final extension (68°C for 5 min). Specific forward (F) and reverse (R) primer pairs were designed by using Primer 3 Software (http://fokker.bpwi.mit.edu/cgi-bin/primer3/primer3_www.cgi): β-actin (F), 5′-GAGAAGATCTGGCACCACACCT-3′; β-actin (R), 5′-CAGGATTCCATACCCAAGAAGG-3′; IFNγ (F), 5′-TGAACGCTACACACTGCATCTTGG-3′; IFNγ (R), 5′-CGACTCCTTTTCCGCTTCCTGAG-3′; perforin (F), 5′-CCGGTCCTGAACTCCTGGCCAC-3′; perforin (R), 5′-CCCCTGCACACATTACTGGAAG-3′; TNFα (F), 5′-TCAGCCGATTTGCTATCTCAT-3′; TNFα (R), 5′-TGAGCCATAATCCCCTTTCTAA-3′; FasL (F), 5′-TCCTTCATTTTCTCGAGGTC-3′; FasL (R), 5′-CGGCTCAGAAAACATTAGGT-3′; COX-2 (F), 5′-GCAAATCCTTGCTGTTCCAATC-3′; COX-2 (R), 5′-GGAGAAGGCTTCCCAGCTTTTG-3′; NKG2D (F), 5′-CACATTGATGTGGCTTGCCATTTT-3′; and NKG2D (R), 5′-AGTTTTTACACCGCCCTTTTCATGC-3′.

All reactions were performed in a 96-well thermocycler (MJ Research PTC-200). Absence of genomic DNA contamination was confirmed by lack of product in control reactions without reverse transcriptase. Sterile, autoclaved water was used as a negative control. Master mixes were used in all reactions to improve accuracy of sqRT-PCR. A total of 6 μl of product from each round of sqRT-PCR (28–40 cycles) was resolved by 1.5% agarose gel electrophoresis at 100 mA for 30 min, and a 100-bp ladder (Invitrogen) was included as a reference for fragment size. DNA was visualized by ethidium bromide by using a UV transilluminator. An image of each gel was taken by using the FluorChem Imaging System (Alpha Innotech, San Leandro, CA) and stored in digitized form. To quantitate relative gene expression, band signal intensities from cycle numbers 36, 38, and 40 were measured by densitometry using Photoshop (Adobe Systems, San Jose, CA) and normalized to the housekeeping gene β-actin.

Real-time qRT-PCR was performed as a service by the W. M. Keck Foundation Biotechnology Resource Laboratory, as described. Briefly, mRNA samples from 500 cell aliquots (isolated by FACS, as above) were converted to cRNA (QantiTECT Probe RT-PCR Kit; Qiagen, Germantown, MD). IFNγ, TNFα, perforin (Prf1), and β-actin primer sets with FAM-based probes (Qiagen), and COX-2 TaqMan primer sets (Applied Biosystems, Foster City, CA) were used to amplify the respective target genes for the TIL and PBL lymphocyte subsets. Samples were run in duplicate on a real-time ABI 7900ht device (Applied Biosystems), and the data were analyzed with provided v2.2 SDS software. For both sqRT-PCR and qRT-PCR analyses, TIL and PBL isolations represent pooled samples from 8–10 tumor-bearing mice. In total, four separate TIL and four separate PBL isolations were performed and analyzed.

Statistics. Statistical significance was evaluated by the two-tailed, unpaired Student *t* test, or nonparametric analysis if standard deviations were significantly different between the two compared groups. Graphical data are shown with bars indicating standard errors of the means.

We thank Gouzel Tokmoulina and Tom Taylor for flow cytometry. We acknowledge the Dermatology Foundation for career support (to M.G.). This work was supported by National Institutes of Health Grants R01 CA102703 (to M.G.) and R01 AR049282 (to R.E.T.), National Institutes of Health/Yale Skin Diseases Research Center Grant P30 AR41942 (to R.E.T.), American Skin Association (B.N.), and the Wellcome Trust (A.H.).

1. Mueller MM (2006) *Eur J Cancer* 42:735–744.
2. Virchow R (1863) *Die Krankhaften Geschwülste* (von August Hirschwald, Berlin), pp 57–101.
3. DePinho RA, Polyak K (2004) *Nat Genet* 36:932–934.
4. Balkwill F, Mantovani A (2001) *Lancet* 357:539–545.
5. Ikeda H, Old LJ, Schreiber RD (2002) *Cytokine Growth Factor Rev* 13:95–109.
6. Girardi M, Oppenheim D, Glusac EJ, Filler R, Balmain R, Tigelaar RE, Hayday AC (2004) *J Invest Dermatol* 122:699–706.
7. He YF, Wang XH, Zhang GM, Chen HT, Zhang H, Feng ZH (2005) *Cancer Immunol Immunother* 54:891–897.
8. Beatty GL, Paterson Y (2000) *J Immunol* 165:5502–5508.
9. Smyth MJ, Cretney E, Kershaw MH, Hayakawa Y (2004) *Immunol Rev* 202:275–293.
10. Philip M, Rowley DA, Schreiber H (2004) *Semin Cancer Biol* 14:433–439.
11. Nickoloff BJ, Ben-Neriah Y, Pikarsky E (2005) *J Invest Dermatol* 1246:10–14.
12. Owens DM, Wei S, Smart RC (1999) *Carcinogenesis* 20:1837–1844.
13. Muller-Decker K, Neufang G, Berger I, Neumann M, Marks F, Furstenberger G (2002) *Proc Natl Acad Sci USA* 99:12483–12488.
14. Tiano HF, Loftin CD, Akunda J, Lee CA, Spalding J, Sessoms A, Dunson DB, Rogan EG, Morham SG, Smart RC, Langenbach R (2002) *Cancer Res* 62:3395–3401.
15. Murakami A, Nakamura Y, Torikai K, Tanaka T, Koshiba T, Koshimizu K, Kuwahara S, Takahashi Y, Ogawa K, Yano M, *et al.* (2000) *Cancer Res* 60:5059–5066.
16. Marks F, Furstenberger G, Neufang G, Muller-Decker K (2003) *Recent Results Cancer Res* 163:46–57, discussion 264–266.
17. Girardi M, Oppenheim DE, Steele CR, Lewis JM, Glusac F, Filler R, Hobby P, Sutton B, Tigelaar RE, Hayday AC (2001) *Science* 294:605–609.
18. Girardi M, Glusac E, Filler RB, Roberts SJ, Lewis J, Tigelaar RE, Hayday AC (2003) *J Exp Med* 198:747–755.

19. Yu P, Lee Y, Liu W, Krausz T, Chong A, Schreiber H, Fu YX (2005) *J Exp Med* 201:779–791.
20. Ghiringhelli F, Menard C, Terme M, Flament C, Taieb J, Chaput N, Puig PE, Novault S, Escudier B, Vivier E, *et al*. (2005) *J Exp Med* 202:1075–1085.
21. Waldmann TA (2006) *Annu Rev Med* 57:65–81.
22. Siegel CT, Schreiber K, Meredith SC, Beck-Engeser GB, Lancki DW, Lazarski CA, Fu YX, Rowley DA, Schreiber H (2000) *J Exp Med* 191:1945–1956.
23. Daniel D, Meyer-Morse N, Bergsland EK, Dehne K, Coussens LM, Hanahan D (2003) *J Exp Med* 197:1017–1028.
24. Fontenot JD, Rasmussen JP, Williams LM, Dooley JL, Farr AG, Rudensky AY (2005) *Immunity* 22:329–341.
25. Ashkar AA, Di Santo JP, Croy BA (2000) *J Exp Med* 192:259–269.
26. Peto J (2001) *Nature* 411:390–395.
27. Prehn RT (1972) *Science* 176:170–171.
28. Moore RJ, Owens DM, Stamp G, Arnott C, Burke F, East N, Holdsworth H, Turner L, Rollins B, Pasparakis M, *et al*. (1999) *Nat Med* 5:828–831.
29. Tiano HF, Loftin CD, Akunda J, Lee CA, Spalding J, Sessoms A, Dunson DB, Rogan EG, Morham SG, Smart RC, Langenbach R (2002) *Cancer Res* 62:3395–3401.
30. Hanada T, Kobayashi T, Chinen T, Saeki K, Takaki H, Koga K, Minoda Y, Sanada T, Yoshioka T, Mimata H, *et al.* (2006) *J Exp Med* 203:1391–1397.
31. Enzler T, Gillessen S, Manis JP, Ferguson D, Fleming J, Alt FW, Mihm M, Dranoff G (2003) *J Exp Med* 197:1213–1219.
32. Schaerli P, Ebert L, Willimann K, Blaser A, Roos RS, Loetscher P, Moser B (2004) *J Exp Med* 199:1265–1275.